

Interest has long since attached to flows in which the bottom region is formed by interaction between several supersonic jets or between a single jet and a wall. This occurs in particular when jets emerge from a set of nozzles arranged around a circle at the bottom of a space, and also in the flow of an annular jet or in a gas-jet compressor with a low ejection coefficient, or when a jet propagates by a step. Most papers deal with the flow for free jets [1-4], and only a few [5] deal with analogous flows for jets near walls. The data on the structures of supersonic jets near walls are quite scanty, and as the flow pattern is very complicated, the most reliable results are provided by experiment [6, 7].

Here is considered the flow of two plane-parallel wall jets near a bottom inlet. The two jets emerge from slot nozzles with sonic velocity, and the distance along the axis between the nozzles may vary widely. The main attention is given to the flow in the initial gas-dynamic part of the jets. A comparison is made with a single wall jet.

1. Figure 1 shows the model of the system used. The jets were injected through slot nozzles along the horizontal walls 1 and 2. The space into which the jets emerged from the nozzles was bounded at the sides by two planar walls, which prevented the jets from leaking sideways and provided a plane-parallel flow structure. The widths  $h$  of the two nozzles were the same at 8 mm. All the geometrical dimensions were normalized to the nozzle width, since it is the definitive parameter in an annular or planar wall jet [7]. The relative distance between the nozzles along the axis  $\bar{\ell} = \ell/h$  varied from 0 to 37.5. The size of the bottom inlet  $\bar{H} = H/h$  was 10.9 in the main series of experiments. The gas flow to the second nozzle was halted to produce a single jet along surface 1.

The pressure ratios  $\bar{p}_0 = p_0/p_\infty$  ( $p_0$  is pressure in the forechamber and  $p_\infty$  is that in the surrounding medium) were 1.9-7.1. The Reynolds numbers derived from the parameters in the exit sections of the nozzles were from  $2.3 \cdot 10^5$  to  $7.7 \cdot 10^5$ . There were drainage holes in the side walls for measurement of the static pressure, which was provided by an automatic data-acquisition system. An IAB-451 apparatus was used to visualize and photograph the flows.

2. When a single underexpanded jet flows along a solid surface, it shows oscillations and alternation of compression and expansion zones. Oblique shock waves arise in the jet, and there is a detached zone at the surface, whose dimensions increase with the total pressure in the jet [6-8]. The length of the first bulge  $S$  in the wall underexpanded jet usually occurs at the distance from the end of the nozzle corresponding to the point at which the first oblique shock wave emerges on the surface of the jet. In a wall jet,  $S$  does not agree with the position of the maximum pressure as measured at the surface [7], so optical measurements are better in determining  $S$ .

In these studies, the dimensions of the first bulge were found by processing schlieren photographs. There is a difference from a free wall jet, for which the self-similar parameter can be taken as the eject factor  $n' = p_a/p_\infty$  ( $p_a$  is the pressure at the end of the nozzle) or  $\bar{p}_0$  [2], in that a jet with a bottom inlet allows only the parameter  $n = p_a/p_b$  ( $p_b$  is the bottom pressure), since the  $n$  may differ greatly for identical  $\bar{p}_0$ , e.g., in the cases of two jets or a single jet. The experiments showed that the relative length of the first bulge was  $\bar{S} = S/h = 4.5$  for  $\bar{p}_0 = 4.3$ , as against 8.5 for two jets. In the two-jet case, if no especial mention is made, we always have in mind the jet closer to the bottom inlet.

Figure 2 shows the  $n$  dependence of  $\bar{S}$  for two jets (open points) and for a single jet (filled points). Points 1-7 correspond to  $\bar{\ell} = 37.5, 25.0, 18.8, 15.9, 9.6, 6.3,$  and  $4.0$ . These data show clearly that  $n$  is the self-similar parameter for a wall jet near the bottom inlet. The distance between the nozzles has hardly any effect on the length of the first bulge. The data gave an expression for the length of the bulge for a planar underexpanded wall jet

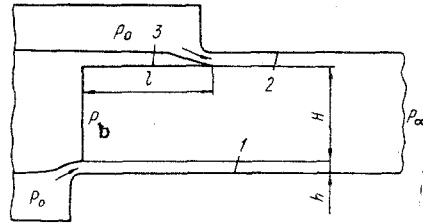


Fig. 1

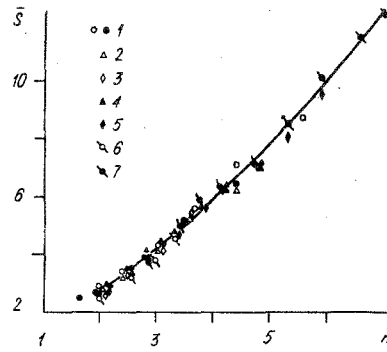


Fig. 2

for  $\bar{p}_0 > 1.9$  and  $M_a = 1$  ( $M_a$  is the Mach number in the exit section of the nozzle), whose error is not more than  $\pm 6\%$ :

$$S/h = 1,17n^{1,20}. \quad (2.1)$$

Figure 2 shows (2.1) as a curve. The behavior of  $\bar{S}(n)$  alters somewhat when a triple shock-wave configuration appears, e.g., in a single jet for  $\bar{p}_0 > 5.6$ , but it still lies within the accuracy given by (2.1). The exponent with the pressure factor for a planar wall jet with bottom inlet is 15-20% larger than for an analogous free jet, in which the length of the bulge is proportional to  $n$  [2] or even to  $n^{1.05}$  [9].

3. As  $p_0$  increases, a single jet propagating around a step with  $\bar{p}_0^* = p_0^*/p_\infty$  becomes completely detached from the surface and adheres to the horizontal wall. A similar picture occurs for two jets, and for  $\bar{l} \neq 0$ , only the jet closer to the bottom inlet becomes detached completely, while the two jets are detached symmetrically for  $\bar{l} = 0$ . For  $\bar{l} \neq 0$ , the jet after detachment interacts either with the nozzle 3 (Fig. 1) or with the second jet in accordance with  $\bar{l}$  (Fig. 3). The separating flow line for the detached jet ends on the second nozzle for  $\bar{l}/H > 1.67$ . When a single jet is detached, the limiting length is reduced and the critical point lies at the nozzle for  $\bar{l}/H > 1.33$ .

The jet detachment is due to the transverse pressure gradient arising from the pressure difference in the detachment zone and bottom region. That difference increases with  $p_0$ , which leads to complete detachment for  $\bar{p}_0 = \bar{p}_0^*$ , when  $(p_b/p_0)^*$  has a quite definite value. Additional experiments for a single jet with various  $\bar{H}$  and unaltered  $\bar{l} = 37.5$  gave an empirical relation for the limiting pressure ratio with an error of  $\pm 5\%$ :

$$(p_b/p_0)^* = 0,463/\bar{H}^{0,605} + 0,3 \cdot 10^{-2}. \quad (3.1)$$

Figure 4 shows (3.1) (line) and the corresponding observed points: 1) for a single jet, and 2) for two jets. The limiting  $(p_b/p_0)^*$  for two jets is less by about 20%. If  $p_0$  is reduced after complete detachment, the initial state is restored for  $\bar{p}_0^{**} < \bar{p}_0^*$ , i.e., there is hysteresis.

Figure 5 shows the  $\bar{l}$  observed dependence of  $\bar{p}_0^*$ ,  $\bar{p}_0^{**}$ , and  $(p_b/p_0)^*$  (points 1-3) for two jets. The second jet reduces the  $\bar{p}_0^*$  required for detachment, and also affects the  $\bar{p}_0^{**}$  at which the jets join up on account of the increased gas ejection from the bottom region and the corresponding reduction in the bottom pressure, which was about 30% less than for a single jet throughout the range in  $\bar{p}_0$ . The form of the curves for a single wall jet is different from those given in Fig. 5 because as  $\bar{l}$  decreases ( $\bar{l}/H < 1.33$ ) for a single jet, there is a size  $\bar{H}$  of the bottom region, while with two jets ( $\bar{l}/H < 1.67$ ), the effective size of the bottom region is reduced. The following empirical relationship fits the measurements for  $(p_b/p_0)^*$  with an accuracy better than 4%:

$$(p_b/p_0)^* = 0,335/\bar{l}^{0,37} - 1/\bar{l}^{2,5} \quad (3.2)$$

(solid line in Fig. 5). The bottom pressure is almost independent of  $\bar{l}$ , so the reduction in  $\bar{l}$  for two jets reduces the pressure difference necessary for complete detachment.

4. The paths of the completely detached jets (axial lines) are shown in Fig. 6 for various pressure differences with two jets ( $\bar{x} = x/h$ ,  $y = y/h$ ). The paths have been con-

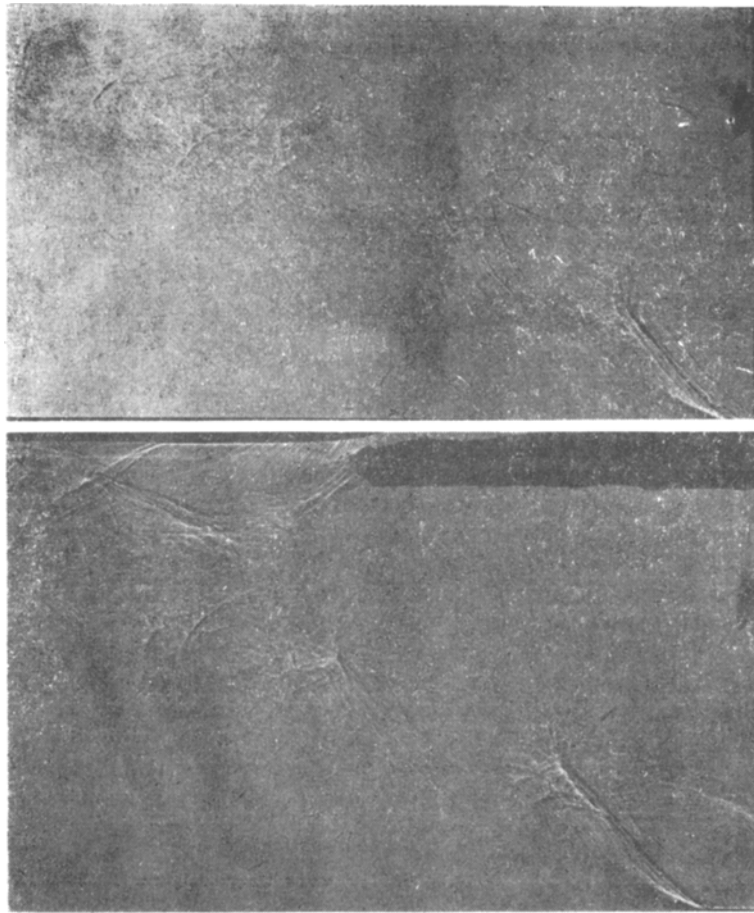


Fig. 3

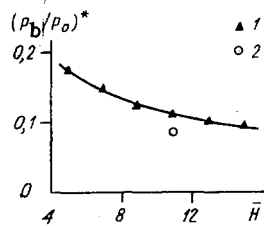


Fig. 4

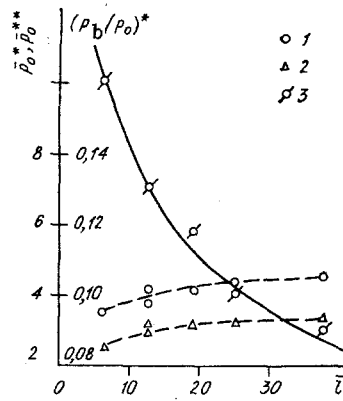


Fig. 5

constructed from schlieren photographs up to the part where the effects of viscosity lead to considerable spread in the jet boundaries and it becomes impossible to determine the paths exactly. For large distances between the nozzles (Fig. 6a,  $\lambda = 25.0$ , lines 1)  $p_0 = 4.90, 5.59, 6.24$ ; 2)  $\bar{p}_0 = 3.61$  in reverse variation), the path of a jet is almost independent of the pressure difference as  $\bar{p}_0$  increases. Changes occur when the pressure is then reduced, namely when  $\bar{p}_0$  is less than  $\bar{p}_0^*$ , with the jet becoming flatter in the initial part, and the critical point approaching the bottom inlet. The longitudinal size of the bottom circulation region is reduced. One can evaluate the change in jet path with  $\bar{p}_0$  qualitatively as follows. We use the equation of motion in projection on the normal  $n_1$  to the jet flow lines  $\rho w^2/r = -\partial p/\partial n_1$  ( $w$  is the total jet velocity,  $\rho$  the density,  $p$  the pressure, and  $r$  the radius of curvature of a flow line), from which we perform simple steps on the basis that the gas speed is

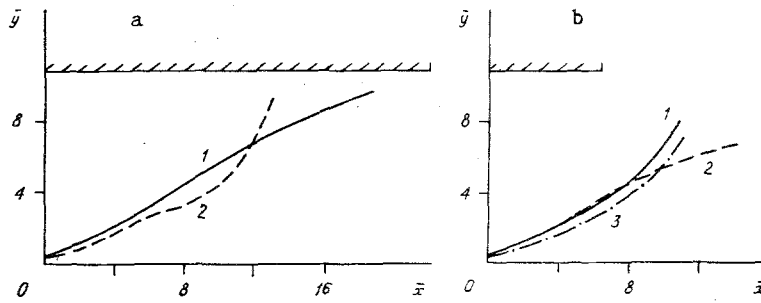


Fig. 6

sonic at the exit from the nozzle and  $\partial p / \partial n_1 \approx (p_b - p_\infty) / \delta$  ( $\delta$  is jet thickness), which gives

$$r = \frac{2\kappa}{\kappa + 1} \varepsilon(1) \delta \frac{1}{\frac{1}{p_0} - \frac{1}{p_b}}$$

Here  $\kappa$  is the adiabatic parameter and  $\varepsilon(1)$  is the gas-dynamic function, which is the ratio of the gas flow density to the density of the halted gas;  $p_b = p_b / p_0$ . We assume that the jet thickness varies little in the pressure difference range used to get

$$r \sim \text{const} \frac{1}{1/p_0 - p_b}$$

The measurements for  $\bar{l} = 25.0$  gave  $1/\bar{p}_0 - \bar{p}_b \approx 0.12$  for  $\bar{p}_0 > \bar{p}_0^*$ , while when the pressure is decreasing, when  $\bar{p}_0^{**} < \bar{p}_0 < \bar{p}_0^*$ ,  $1/\bar{p}_0 - \bar{p}_b$  alters, since  $\partial \bar{p}_b / \partial \bar{p}_0$  is substantially increased, which affects the radius of curvature.

When the distance between nozzles is short (Fig. 6b,  $\bar{l} = 6.3$ , lines 1)  $\bar{p}_0 = 3.61$ ; 2) 5.59; 3) 2.95 for reverse course), the path of a detached jet varies with the pressure difference during increase and decrease, which is due to interaction between the two jets.

After the wall jet has become detached and the pressure difference is increasing further, the bottom region is shut off at a certain  $p_0^+$ , and then the relative bottom pressure  $p_b$  is independent of  $p_0$ . With a single jet, that state arises only for  $H \leq 4.9$  on account of the lateral interaction between the underexpanded jet and the horizontal screen. A strong oblique shock wave hinders further jet expansion. The bottom region is isolated from the conditions occurring downstream.

When there are two jets, a closed bottom region occurs also for large  $\bar{H}$ . That region is confirmed for  $\bar{H} = 10.9$  from the presence of a part having  $p_b = \text{const}$  on  $p_b(p_0)$  and by the distribution of the relative static pressure  $\bar{p} = p/p_0$  along the nozzle, which in that state is independent of  $p_0$ . A closed region is formed with large distances between the nozzles ( $\bar{l}/H > 1.67$ ) because of interaction between the supersonic part of the jet and the side of the nozzle, while for small  $\bar{l}$ , it occurs on account of interaction between the supersonic parts of the two jets. When the bottom region has been shut off, it is surrounded by a supersonic flow, and the pressure in it is independent of the pressure in the surrounding space and varies in proportion to the total jet pressure  $p_0$ . Then  $p_0^+$  increases as  $\bar{l}$  decreases in accordance with the empirical relationship  $\bar{p}_0^+ = 8.01/\bar{l}^{0.13}$ .

#### LITERATURE CITED

1. G. N. Abramovich, T. A. Girshovich, S. Yu. Krashenninikov, et al., Turbulent Jet Theory, G. N. Abramovich (ed.), 2nd edn. [in Russian], Nauka, Moscow (1984).
2. V. S. Avduevskii, É. A. Ashratov, A. V. Ivanov, et al., Gas Dynamics of Supersonic Non-isobaric Jets [in Russian], Mashinostroenie, Moscow (1989).
3. A. I. Shvets and I. T. Shvets, Near-Wake Gas Dynamics [in Russian], Naukova Dumka, Kiev (1976).
4. M. A. Koval' and A. I. Shvets, "An experimental study on sonic and supersonic ring jets," Prikl. Mekh. Tekh. Fiz., No. 4 (1974).

5. M. M. Nazarchuk and V. N. Panchenko, Bounded Jets [in Russian], Naukova Dumka, Kiev (1981).
6. L. N. Lebedeva and V. V. Filatov, "A study on a sonic underexpanded jet flowing from a slot along a surface," *Izv. Vyssh. Uchebn. Zaved., Aviats. Tekhnika*, No. 3 (1983).
7. Yu. Ya. Borisov and S. A. Podol'skii, "Bulge length in an annular underexpanded jet flowing from a sonic nozzle having a cylindrical rod at the axis," *Izv. Akad. Nauk SSSR, MZhG*, No. 4 (1980).
8. E. G. Zaitsev, "Effects from the displacement of high-pressure gas along the nozzle axis on ejector shut-off conditions," *Trudy TsAGI*, Issue 2458 (1989).
9. W. J. Sheeran and D. S. Dasanjh, "Observation of jet flows from a two-dimensional under-expanded sonic nozzle," *AIAA J.*, 6, No. 3 (1968).

INFLUENCE OF THERMAL EFFECTS ON HYDRODYNAMIC STABILITY OF A  
POLYMERIZATION FRONT

G. V. Zhizhin and A. S. Segal'

UDC 532.5:541.64

Two features are usually distinguished in investigating the stability of fronts of chemical reactions: diffusive-thermal and hydrodynamic stability [1]. The diffusive-thermal stability is analyzed under the assumption that perturbations of the front shape are not accompanied by perturbations of hydrodynamic fields in its vicinity [2], while the hydrodynamic stability is analyzed under the assumption that, on the contrary, no perturbations of the concentration and thermal fields are generated [3]. The last assumption is justified if the front width  $\delta$  is negligibly small in comparison with the perturbation wavelength  $\lambda$  (the zeroth approximation in the small parameter  $\varepsilon = \delta/\lambda$ ). For short-wave perturbations ( $\delta \sim \lambda$ ) it is necessary to take into account the simultaneous occurrence of diffusive-thermal and hydrodynamic processes. This account was carried out most consistently in [4], as applied to a planar front in the gas phase. The analysis is restricted to the first approximation in  $\varepsilon$ , using an asymptotic method of solving singular perturbation problems with a surface discontinuity, as developed in [5].

The problem of creating a continuous technological process of obtaining polymer materials on the basis of the polymerization frontal effect [6] leads to the statement of stability problems of cylindrical and spherical polymerization fronts in radial flows. An important polymerization effect is a strong increase in medium viscosity; therefore, the hydrodynamic stability analyzed in [7, 8] is of basic interest in the given case. The thermal stability investigated in [9] for a cylindrical front is unrelated to any new physical effects relative to [2].

In the present study we consider the stability of a stationary cylindrical front in a radial flow with account of the mutual effect of thermal and hydrodynamic effects. The analysis is carried out within the first approximation in  $\varepsilon$  by the method of matched asymptotic expansions, in which case, unlike [4], one uses the convenient method of transition to a moving curvilinear natural coordinate system attached to the front [10]. First order corrections in  $\varepsilon$  to the solution obtained in [7] are found, and their effect on front stability is analyzed.

1. We restrict ourselves to the case of angular perturbations of a cylindrical front, in which case the problem can be considered as planar in the cross section normal to the front axis. Let the closed front  $F$  be located between two penetrable coaxial cylindrical surfaces  $S_-$  and  $S_+$ , and let it propagate in the direction of the normal  $n$  toward the flow (the internal supply of the medium), with the regions  $\Omega_-$  and  $\Omega_+$  filled by the original mixture and by the final product (see Fig. 1). Following [2, 4], the problem is solved in the zeroth approximation in the small Frank-Kamenetskii parameter  $\beta = \bar{R}T_r/E$  ( $\bar{R}$  is the universal